

DUST-CHARGING PROCESSES IN PLASMA ENVIRONMENTS

REBECCA A. ROBINSON

Colorado Center for Lunar Dust and Atmospheric Studies
University of Colorado at Boulder, Boulder, Colorado
Sascha Kempf, PhD and Mihaly Horanyi, PhD

August 12, 2012

ABSTRACT

The Cosmic Dust Analyzer aboard the Cassini spacecraft consists of a several targets as well as a photomultiplier tube which provide information upon collision with ambient dust particles in Saturn's magnetosphere. Information includes particle mass, velocity, chemical composition, and charge. The focus of this report is the charge of the dust particles; specifically, the processes by which these particles may be charged. Grain charging in such an environment is dominated by four specific currents: electron currents, ion currents, photoelectron currents produced by ultraviolet radiation, and secondary electron currents caused by the bombardment of the grain by energetic particles. Simulations of Saturnian plasma environments were analyzed and compared to data from the CDA. The dependence of both equilibrium potential and charge on grain size was also explored.

1. INTRODUCTION

1.1. *Space Plasmas and Magnetospheres*

Several planets in our local solar system are surrounded by extensive magnetic fields that extend several planetary radii away from their respective planets. Such environments provide the necessary conditions for many physical events to occur, therefore making them excellent laboratories in and of themselves. Processes spanning the entire spectrum of physics are present here, including but of course not limited to electromagnetism, particle and nuclear physics, thermodynamics, and kinematics. Cosmic rays, gamma rays, and ultraviolet radiation provide the energy required to ionize the gasses in magnetospheres, thus creating an ambient plasma environment.

For simplicity, scientists often model planetary magnetic fields as perfect dipoles centered on the planet. However, interactions with the solar wind and other particles create several perturbations to the perfect dipole model; most prominently, the magnetic tail. The tail is formed by collisionless energy and momentum transfers from the solar wind, which extend the far side of the magnetosphere with respect to the sun (Parks 1991). Other magnetospheric features include the magnetosheath which encompasses the outer sunward magnetosphere, the bow-shock region which encompasses the magnetosheath, the magnetopause which separates the magnetosheath from the boundary of the magnetic tail, and the plasmashield which is essentially the middle of the magnetic tail (Figure 1). Such magnetic structures are observed not only around planets but around stars as well; even entire galaxies have enormous magnetospheres!

1.2. *Saturnian Magnetosphere and Grain Charging*

In 1979, the spacecraft Pioneer 11 discovered the magnetosphere of Saturn via the observation of its bow-shock region, and instruments aboard Voyagers 1 and 2 continued the study (van Allen 1984). In 1997, the spacecraft

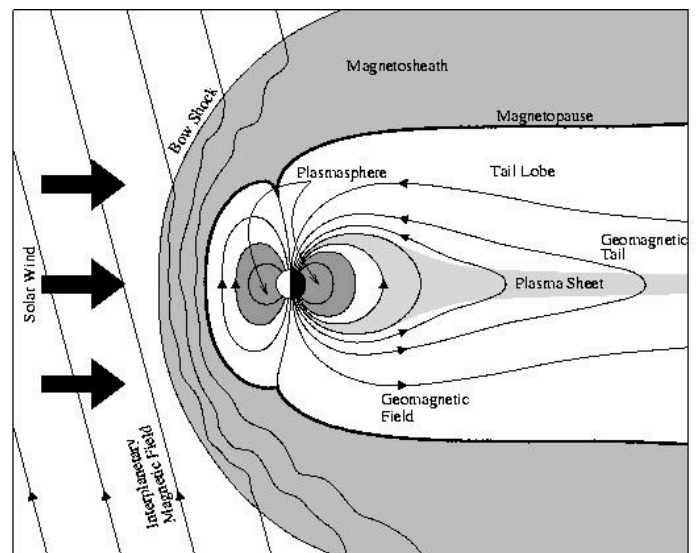


FIG. 1.— Diagram of Earth's magnetosphere in order to illustrate the many different parts of magnetic environments. (from Umea Universitet, tp.umu.se)

Cassini was launched and after seven years and a quick stop in the Jovian system, it reached the Saturnian system (Kempf et al. 2006). Since then, the instruments on board Cassini have provided a wealth of information regarding the Saturnian system. Aside from measurements of the magnetic field, the aforementioned instruments have also observed several different ion and electron currents present in the Saturnian magnetosphere, including H^+ ions, O^+ ions, hot electrons (low density, high energy), and cold electrons (high density, low energy) (Horanyi 1996). Micron-sized grains in the Saturnian ring system readily interact with the magnetic field as well as the charge currents listed above. Such currents, however, are not limited to electrons and ions. There are four observed currents that are responsible for the charging-up of the micron-sized grains in the magnetosphere: electron current (Equations 1 and 2), ion current (Equations 3 and 4), photoelectron current (Equations 5

and 6), and secondary electron current (Equations 7-11). The electron and ion currents, described by nearly identical equations, are simply currents comprised of either electrons or ions. The photoelectron current is only relevant on the sunward side of the magnetosphere because it is a current of photoelectrons excited via ultraviolet radiation from the sun. Similarly, the secondary electron current is relevant whenever particles are excited enough by primary currents to produce a secondary current of electrons (Horanyi 1996). The sum of these four currents together gives the total charge current for the Saturnian environment, which of course, is equal to the time derivative of charge (Equation 12). By solving the differential equation for charge, we can use Equation 13 in order to solve for the equilibrium potential of the Saturnian environment. The Cosmic Dust Analyzer (CDA) instrument aboard Cassini collects this information upon collision with charged grains. The CDA detector consists of a rhodium target (for chemical analysis of the grain), entrance grids and impact targets, and a photomultiplier tube (Srama et al. 2004). Grain collisions with the CDA provide information regarding the mass, velocity, chemical constituents, and charge of the grain. This report focuses mainly on the grain charge as well as the charging processes.

1.3. Equations

Electron Current:

$$J_e = 4\pi a^2 n_e \sqrt{\frac{kT_e}{2\pi m_e}} e^{\frac{-e\phi}{kT_e}} (if \frac{-e\phi}{kT_e} \geq 0) \quad (1)$$

$$J_e = 4\pi a^2 n_e \sqrt{\frac{kT_e}{2\pi m_e}} (1 - \frac{-e\phi}{kT_e}) (if \frac{-e\phi}{kT_e} < 0) \quad (2)$$

Ion Current:

$$J_i = 4\pi a^2 n_i \sqrt{\frac{kT_i}{2\pi m_i}} e^{\frac{e\phi}{kT_i}} (if \frac{e\phi}{kT_i} \geq 0) \quad (3)$$

$$J_i = 4\pi a^2 n_i \sqrt{\frac{kT_i}{2\pi m_i}} (1 - \frac{e\phi}{kT_i}) (if \frac{e\phi}{kT_i} < 0) \quad (4)$$

Photoelectron Current:

$$J_v = \frac{2.5 \times 10^{14} \kappa}{d^2} \pi a^2 (if \phi < 0) \quad (5)$$

$$J_v = \frac{2.5 \times 10^{10} \kappa}{d^2} \pi a^2 e^{\frac{-e\phi}{kT_v}} (if \phi \geq 0) \quad (6)$$

Secondary Electron Current:

$$J_s = 3.7\delta_m (4\pi a^2 n_e \sqrt{\frac{kT_e}{2\pi m_e}} e^{\frac{-e\phi}{kT_e}} F_5(\frac{E_m}{4kT_e})) (if \phi < 0) \quad (7)$$

$$F_5(x) = \int_0^\infty u^5 e^{-(xu^2+u)} du \quad (8)$$

$$J_s = 3.7\delta_m (4\pi a^2 n_e \sqrt{\frac{kT_e}{2\pi m_e}} (1 - \frac{-e\phi}{kT_s}) e^{\frac{-e\phi}{kT_s} - \frac{-e\phi}{kT_e}} F_{5,B}(\frac{E_m}{4kT_e})) \quad (9)$$

(if $\phi > 0$)

$$F_{5,B} = \int_B^\infty u^5 e^{-(xu^2+u)} du \quad (10)$$

$$B = \sqrt{\frac{4(kT_e)^2}{E_m e \phi}} \quad (11)$$

Total Charge Current:

$$\frac{dQ}{dt} = \Sigma J(\phi(t)) = J_e(\phi(t)) + J_i(\phi(t)) + J_v(\phi(t)) + J_s(\phi(t)) \quad (12)$$

Potential:

$$\phi = \frac{Q}{4\pi\epsilon_0 R} \quad (13)$$

2. PROCEDURE

2.1. Algorithm

A charge-current algorithm was developed using IDL, ultimately in order to compute equilibrium potentials of specific plasma environments. This algorithm takes into account the electron/ion currents as well as the photoelectron current; however, it does not account for secondary electron currents. The code uses the Runge-Kutta method in order to solve Equation 12 for Q, and then using Equation 13, computes the equilibrium potential of the environment and creates a plot of current vs. time. Once the code was written, I was able to play around with the variable parameters such as current energy, plasma density, distance of the grain from the sun, grain size, etc. First, a sample environment taken from (Horanyi 1996) was used in order to test the legitimacy of the code. Then, a Saturnian environment was simulated based on several parameters given in (Horanyi 1996). Equilibrium potentials were computed in each case, and the grain size dependence of both potential and charge was found and compared to trends evident in CDA data.

2.2. CDA Data

A subset of the plasma UV data from the Cosmic Dust Analyzer was explored. A total of 1572 charge signals, as detected by the CDA, were defined. The interface developed for the analysis of CDA data defined several characteristics of each charge signal. These characteristics include velocity, charge, potential, position in the Saturnian system, position of collision on the detector itself, grain size, and dust trajectory. Using these individual and collective grain properties, comparisons were made to the results from the simulations.

3. ANALYSIS

3.1. Plasma Simulations

The test environment for the charge-current code was incredibly simple. It was comprised of 10eV electrons and ions with equivalent densities as well as 2eV photoelectrons which bombarded a micron-sized grain located at a distance of one astronomical unit (one Earth distance) from the sun. From these initial parameters, the code gave an equilibrium potential of 1.48V. Although this is smaller than the expected value by roughly a factor of 3, it is a reasonable result.

A hot-electron, hydrogen ion environment was then simulated at a distance of 9.5 astronomical units from the sun, which is the distance between Saturn and the sun. This environment is similar to the environment around Saturn's moon Enceladus, although cold electrons, that are known to be there, were not included in this model. The hot electrons exist in a low-density environment ($0.2 \times 10^6 \text{ m}^{-3}$) which corresponds to their high energies (100eV), and we assume that the hydrogen ions have a density of $10 \times 10^6 \text{ m}^{-3}$ and an energy, as in the test environment, of 10eV (Horanyi 1996). In this case, the energy of the hot electrons dominates the charge current and, hence, dominates the charge and potential as well. As expected, the code returned a negative potential value of -2.4V. It is worthy to note that the boundary between negative and positive potential values in the Saturnian environment is located at about 8 Saturn radii, near the moon Rhea and the boundary of the E Ring (Kempf et al. 2006). Since Enceladus is located at 4 Saturn radii, well inside the orbit of Rhea, we expect a negative potential value. From (Horanyi 1996), the expected potential value should actually lie within the range of $-8\text{V} < \phi < -4\text{V}$; however, since my code does not take into account the cold electrons, oxygen ions, or secondary electron current, a returned value of -2.4V seems reasonable.

The equilibrium potential for the Saturnian hot-electron and hydrogen-ion environment was computed for varying grain radii in order to plot the dependence of both potential and charge on varying grain size. Figures 2 and 3 clearly show that both charge and potential values decrease with increasing grain radius. Linear models were applied to both potential vs. grain size and charge vs. grain size. The model $y = -0.97727272x - 3.0363939$, with an R^2 value of 0.943329, was applied to potential vs. grain size whereas the model $y = -1.670944x + 2.7753027$, with an R^2 value of 0.988384, was applied to charge vs. grain size (Figures 4 and 5). These relationships are completely intuitive; it takes longer to charge a larger particle. For such large particles, dQ/dt is smaller than it would be for smaller particles; therefore, Q is smaller and by extension, ϕ is smaller.

3.2. Comparison with CDA Data

Analysis of the CDA data confirmed the relationship between potential and grain size as well as the relationship between charge and grain size (Figures 6 and 7). Furthermore, the majority of the data points in this particular data set were located around 4 Saturn radii as shown in Figure 8 and returned a negative potential value, as expected. However, there are still some points of ambiguity that would be worth exploring in the future. The data and the simulations agree on basic grounds, but the correlation can likely become more strong with further development of the IDL code and analysis of the validity of the CDA charge signals. Things to take into account with regards to the simulation are: addition of the secondary electron current (since a high-energy hot-electron environment would stimulate secondary electrons), addition of O^+ ions and others (since this environment is known to contain water, sodium, etc. (Horanyi 1996)), and addition of cold electrons. As for

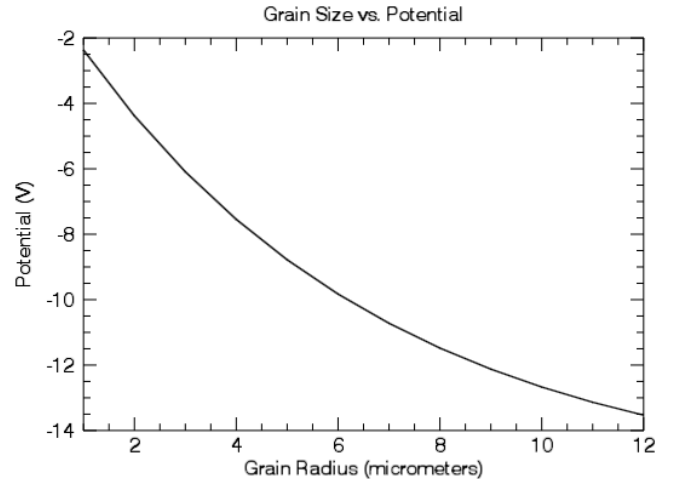


FIG. 2.— Plot of potential in volts vs. grain size in μm

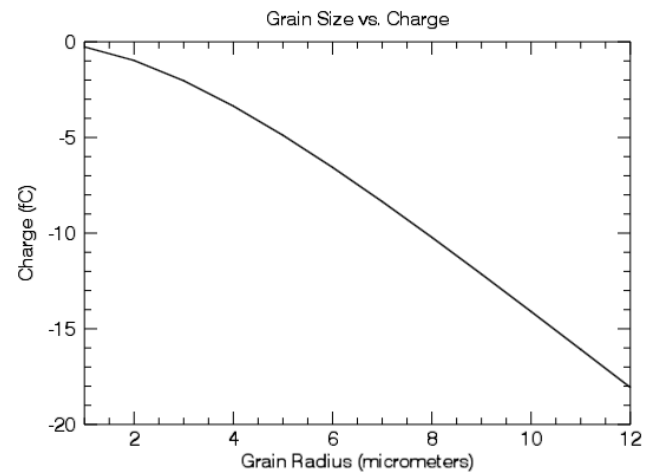


FIG. 3.— Plot of charge in fempto-Coulombs vs. grain size in μm

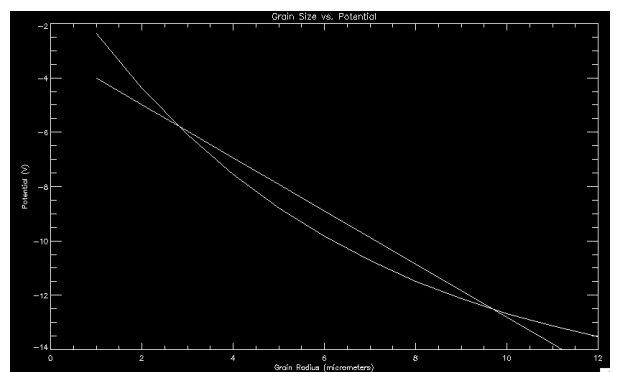


FIG. 4.— Linear fit for ϕ vs. grain size, $R^2=0.943329$

the data, it would be helpful to know at what point certain signals, for example those that give potential values of 0V, may be thrown out so that the statistics describing the overall Saturnian environment might be more accurate.

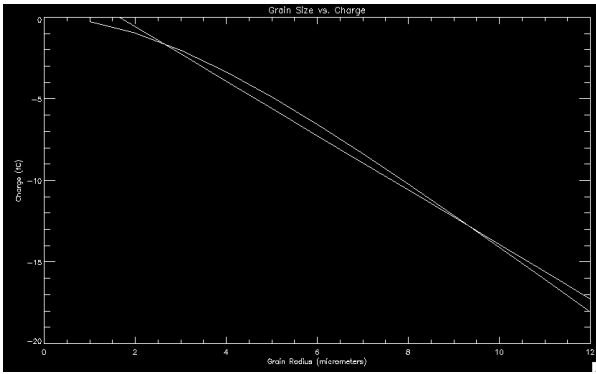


FIG. 5.— Linear fit for charge vs. grain size, $R^2=0.988384$

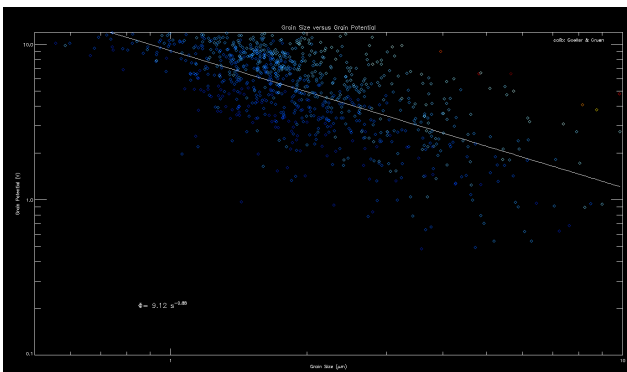


FIG. 6.— Plot from CDA data set of phi vs. grain size. The data show a decreasing trend, as expected.

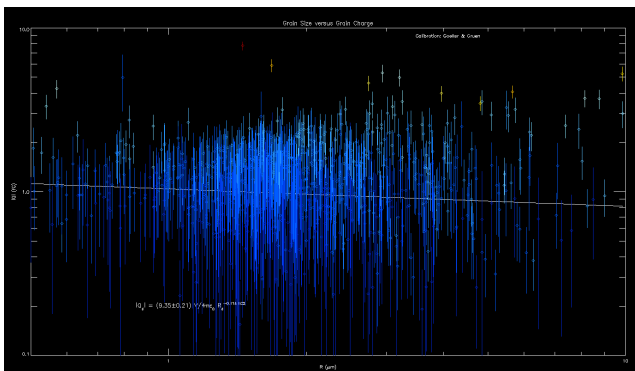


FIG. 7.— Plot from CDA data set of charge vs. grain size. The data show a decreasing trend, as expected.

4. CONCLUSION

Simulations of a Saturnian plasma environment were run for a hot-electron and hydrogen-ion environment similar to the environment surrounding the moon Enceladus.

REFERENCES

- Horanyi, M. 1996, ARA&A, 34, 383
 Kempf, S., Beckmann, U., Srama, R., et al. 2006, Planet. Space Sci., 54, 999
 Parks, G. K. 1991, Redwood City, CA, Addison-Wesley Publishing Co., 1991, 547 p.,

An equilibrium potential value of $-2.4V$ was computed. This negative value is expected for a particle in the vicinity of Enceladus. The same environment was run again several times with only varying grain size to test the relationships between potential and grain size as well as charge and grain size. It was found that both potential and charge decrease linearly with increasing grain size, which was confirmed using CDA data. For future analysis, it would be necessary to take into account the secondary electron current, other ion current sources, and cold electrons. Also, in order to improve the statistics of the overall data set, outliers need to be identified and set

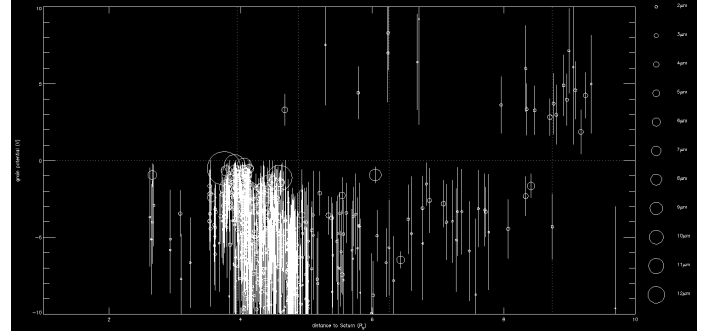


FIG. 8.— Plot of potential in volts vs. distance from Saturn in Saturn radii, as well as grain size denoted by circle radius. The concentration of points in this data set centers around roughly 4 Saturn radii, which corresponds to the orbit of the moon Enceladus. Here, the equilibrium potential of each grain should be negative, as shown in the plot.

aside. As the simulation currently stands, results agree with the data set. However, the addition of known parameters might strengthen the agreement between the simulation and the data and would provide the opportunity for the accurate testing of other Saturnian plasma environments.

The author wishes to acknowledge Dr. Mihaly Horanyi and Dr. Sascha Kempf for the opportunity to work on this project, as well as NASA's Jet Propulsion Lab, ESA, and the Cassini Team. She also wishes to thank Deborah Jin, Leigh Dodd, and Dan Dessau for their organization of the REU program, Dr. Anna Mocker and Leela O'Brien for their continued support, and her fellow research students for their enthusiasm and encouragement. She is grateful to the National Science Foundation for providing the necessary funds for her work.